AN EFFICIENT APPROACH FOR BRAIN TUMOUR DETECTION AND CLASSIFICATION IN MULTI-MODEL MR BRAIN IMAGES USING RPCA AND QT DECOMPOSITION FUSION AND ANN CLASSIFICATION TECHNIQUE

[1]Padmanjali A Hagargi, [2]Dr. Shubhangi DC
[1]Asstant Professor, [2]Professor
[1]Departmewnt of Information Science and Engineering,
[1]Guru Nanak Dev Engineering, Bidar, India

Abstract: An important imaging technique that used to identify the brain tumor is magnetic resonance imaging (MRI). One of most dangerous diseases occurring among adults and children is brain tumor. As there is an apparent chance in survival of patients if tumor identified in the early stage, automatic approach of image classification is an emerging research area in the medical field. These are the reasons motivated our approach of machine learning. Here we presented efficient tumor detection and its classification approach using efficient fusion techniques and segmentation algorithms. In the proposed system pre-processing block includes wiener filtering that removes the noisy pixels from the image. We have involved fusion of T1 and T2 slices of MRI image for efficient tumor detection. By using techniques like RPCA and QT decomposition for Image fusion, Level Set Segmentation to detect the tumor region, feature extraction techniques like GLCM and Gray Level Run Length Matrix (GLRLM). Along with ANN classifier for classification, we have reached to accuracy of about 93.4 for our proposed method.

IndexTerms - RPCA and QT decomposition, Level Set Segmentation, GLCM, GLRLM, ANN.

I. INTRODUCTION

Brain is a delicate, soft, spongy and non-replaceable mass of tissue. Tumor is large mass of tissues; they grow out of control of the normal forces that controls the growth. The tumor in Brain is nothing but a group of abnormal cells they grow around or within the brain. Tumors have the capability to destroy all the cells which are healthy. Tumor can also damage indirectly the existing healthy cells by joining other parts of the brain and causing inflammation brain swelling, inflammation and pressure inside the skull. Over the last twenty years, overall incidence of cancer, including brain cancer, has increased by more than10%, as reported in the National Cancer Institute Statistics (NCIS). The National Brain Tumor Foundation (NBTF) is the research centre in the U.S gives the estimation of about 29,000 people in the U.S are identified with suffering from primary brain tumors every year and about 13,000 people are found dying.

In children, one quarter of deaths of cancer is because of the tumor in brain. The overall yearly incidents of the initial brain tumors in the U.S is about 11 to 12 people per 100,000 people and for primary malignant tumors, that rate is about 6 to 7 people per 1,00,000 people. In the U.K the people more than 4,200 are identified with the brain tumor annually (2007 estimates). More than 200 types of tumor identification is done every year in U.K. About 16 out of every 1,000 cancers diagnosed in the U.K are in the brain (or 1.6%). In India, more than 80,271 persons are affected with various types of tumor.

One among the oldest tools used during disease diagnosis and treatment of these kinds of diseases is MRI. This modality of imaging produces images of soft tissue. The captured medical images show the internal structure, but the doctors want more than the peer images to depict the information's like finding abnormal tissue, shape and so on. If such observations are covered by the doctors themselves, chances to be inaccurate are more and are very time consuming. Hence using an efficient segmentation is necessary to get accurate result by detecting and extracting tumor region in MRI images.

The tumor is same for the word neoplasm, which is formed by the abnormal growing of the tumor cells which is different from the cancer. Usually there are 2 types of the tumor: Benign; Malignant. The tumor which doesn't expand in the abrupt way is a benign type of tumor. It does not affect the neighboring tissues which are healthy. Malignant tumor is the type of tumor that grows with the passage of time and worsens the situation leading to death. This disease is a severe progressing disease. This disease leads to the cancer usually. Hence enormous research has been carried in the recent years for the efficient segmentation and the tumor classification in the given MRI of the Tumor in the brain.

In our proposed method, the pictorial information of 2 slices of MRI imaging; T1 and T2 are integrated that will provide the extended information about the brain internal structuring. Based on this information tumor sections are segmented from image by making use of the level set segmentation. The necessity for classification of segmented images into tumor or non-tumor sections is provided by feature vectors. Features are accumulated by decomposing images using RPCA and Quad tree, and then building features using GLCM, GLRLM, PHOG and CLBP methods. Classification is dependent on these feature vectors and ANN classifier has finally made efficient tumor classification into benign and malignant.

II. LITERATURE SURVEY

Mohammad Havaei et.al [01] presented a fully automatic brain tumor segmentation approach using DNNs (Deep Neural Networks). This work considered both high and low grade pictures in MRI. An efficient CNN based architecture which is different from the traditional technique is made use in the computer vision. Proposed CNN in this work exploits both the local features and the contextual global features simultaneously. To tackle the difficulties caused because of the imbalance of the tumor labels two phase training method is allowed. The evaluation of the algorithm is done on the BRATS test dataset.

Bjoern H. Menze et.al [02] reported the set up along with results of BRATS (Multimodal Brain Tumor Image Segmentation Benchmark). Reviews on different state- of -art work has been done and also it is found that the different algorithms are worked best for different sub regions, but none of the algorithms had ranked in top for all the sub regions simultaneously. Hence fusing of several algorithms which are good using a hierarchical segmentation approach based on majority yielded Vote that ranked consistently above all the individual algorithm is done.

. Nelly Gordillo et.al [03] presents overview of more relevant segmentation of the brain tumor methods that are conducted after the image acquisition. Advantages of MRI is given over other imaging diagnostic, the survey is focused more on the MRI tumor segmentation. Semi automatic and fully automatic techniques are emphasized. Xavier Llado et.al [04] has proposed an efficient method for MS lesion segmentation. This paper, reviewed main approaches of the automated MS segmentation of lesion. The main segmented features are studied and more recent good techniques are classified into the different strategies based on their main principle, point out their strengths and the weaknesses and then suggesting the new research directions. A qualitative and quantitative comparison of results of approaches analyzed is also presented.

M.H. Fazel Zarandi et.al [05] has presented a systematic type 2 system of fuzzy for identifying the cancer of human brain (Astrocytoma tumor) by using T1-weighted MRI with contrast. In this approach Type 2 fuzzy processing approach has mainly four different modules: Feature Extraction, Segmentation, Pre-processing and the Approximate Reasoning. We develop the fuzzy based rule by performing aggregation on the already existing filtering techniques for the steps of Pre-processing. For the next step of Segmentation, they then extend the Possibilistic C-Mean (PCM) procedure by using Type 2 fuzzy methods, Kwon validity index, and Mahalanobis distance. Extraction of the Feature is done by making use of the Thresholding technique. They have later developed a Type 2 Approximate method of Reasoning for the reorganization of the tumor grade in brain MRI. Type-II expert system is tested and validated in real world to show the accuracy. The results shows that this approach is superior in recognizing the brain tumor and its grade than Type-I fuzzy expert systems.

El-Sayed Ahmed El-Dahshan et.al [06] presented the hybrid technique to classify the MRI. This hybrid approach usually consists of the 3 stages, namely, dimensionality reduction, feature extraction and then classification step. In the first stage they have extracted the features that are relevant to MRI images byusing DWT (discrete wavelet transformation). In the second stage, reduction in the features of the MR images is done by the principal component analysis (PCA), to more essential features. In classification process, development of two classifiers is done. The 1st classifier is based on the feed forward back propagation artificial neural network (FP-ANN) and the 2nd classifier is based on the k nearest neighbour (k-NN). The classifiers are used to classify the subjects as the abnormal or normal MRI human images.

T. Logeswar et.al [07] proposed an efficient method for Image Segmentation. In this paper an efficient technique for the clustering using a SOM (Self Organizing Map) algorithm is proposed for the segmentation of the medical image segmentation. This paper mainly describes that segmentation method mainly focused on 2 phases. In the 1st phase, the MRI image of brain the patient is acquired from patient database and then from this film noise and artifacts are removed. In the 2nd phase segmentation of MR they have identified the principal structures of the tissues in these images. This paper also included the study on checking the statistical feature efficiency using Gabor Wavelet feature extraction technique and classification using several classifiers.

Kailash Sinha et.al [08] did a study on methods k-means clustering combined with watershed algorithm of segmentation algorithm, optimized k-means clustering combined with genetic algorithm and also optimized clustering of the c- means combined with the genetic algorithm. Sensitivity of Traditional k-means algorithm to central clusters is utilized with Genetic c-means for the brain tumor detection. Among all three genetic c-means is considered as better performer as it not only eliminated over segmentation sectors, also provided efficient results for clustering.

Nooshin Nabizadeh et.al [09] proposed a model that delineates the tumor sector automatically on T1-w and FLAIR types. The advantage of the method is that working on single slice made the work easier and cost effective with no registration policy. Gabor wavelets and statistical features are the main building blocks of the method. The comparison between two concluded statistical features as the better accuracy based method; sufficient feature collector for T1 and FLAIR images on other hand Gabor wavelet is more memory consumer, highly redundant and costly.

Manavalan Radhakrishnan et.al [10] proposed work for TRUS prostate images. Statistical parameters are calculated for analysis of classifier performance such as; sensitivity, specificity and accuracy. The comparison of features sets is done here by examining the individual based features results and combined feature results. Histogram and GLRLM features are giving poor performance and histogram, GLRLM and GLCM combined features stood well for the classification. Researchers in [11], [12], [13], [14], [15], [16], [17], [18], [19], [20], [21], [22], [23], [24], [25] are also proposed an efficient techniques for tumor detection. In the proposed methodology for efficient tumor detection in the entire input query MRI images using efficient techniques like RPCA and QT decomposition for Image fusion, Level Set Segmentation to detect the tumor region, feature extraction techniques like GLCM and Gray-Level Run-Length Matrix (GLRLM) Along with ANN classifier for classification of final result on tumor or non tumor.

III. METHODOLOGY

The proposed diagram is as shown in Fig. 1. It consists of two phases called testing phase and the training Phase. In the testing phase initially the input MRI images T1, T2 are passed to the pre-processing block. In pre-processing, different pre-processing steps like resizing, RGB to Grayscale conversion and the noise removal also done. Resizing step includes changing size of input to some fixed size. In the noise removal step noise removal using the filter called Wiener is made use. Once the T1 and T2 images are filtered both the images are passed to image fusion block. In the fusion block both these images are then decomposed to get the fused image using RPCA and QT decomposition.

The obtained fused image then passed to feature extraction block. Technique like level set segmentation is used to detect the tumor region. Segmented region may contain tumor or non-tumor region, hence extracting the appropriate features from it is very necessary to find the exact tumor region. Prominent features from these segmented regions are extracted using GLCM and GLRLM techniques. The extracted features then passed to ANN classifier. In training phase segmented tumor image samples taken as the input and are passed to pre-processing block to follow the same steps as carried in the testing phase. Features from these samples are extracted and stored in the knowledge base. Every time during the classification the extracted features from the query image is compared with the features already stored in the knowledge base to classify if the query image contains disease or not.

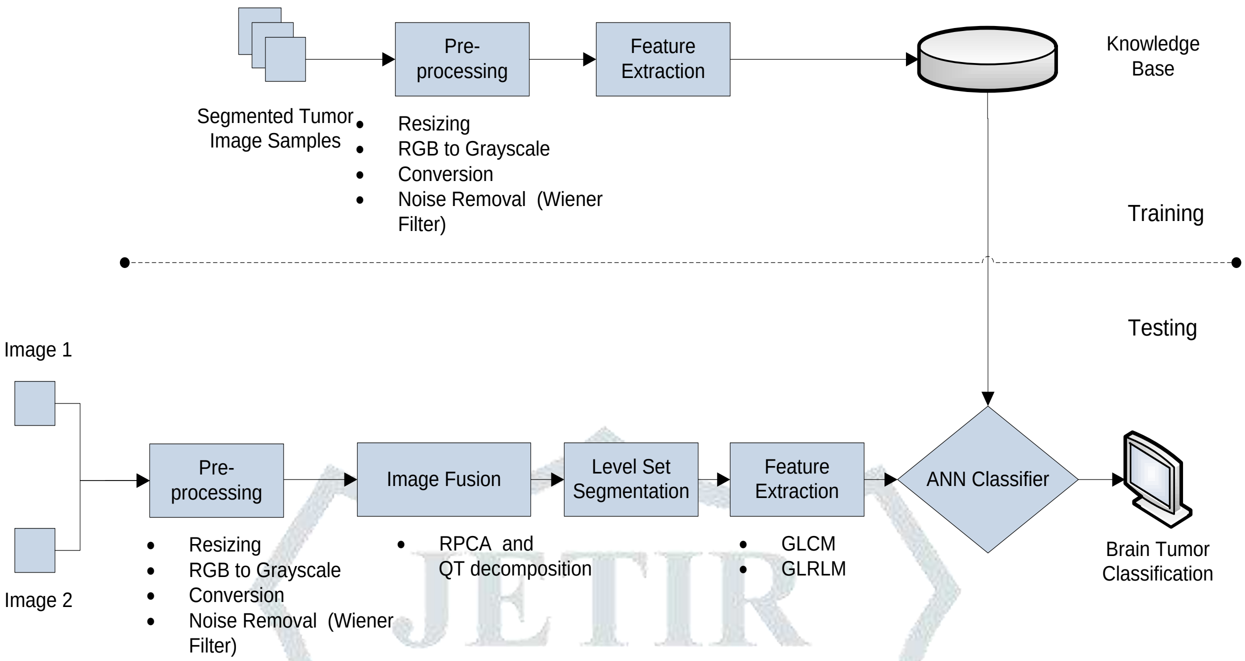

Fig. 1: Block Diagram of the Proposed System

3.1 **Pre-processing**

Usually the patient MRI images obtained will be two dimensional units. But usually these images will be of different sizes. Hence these images are fixed into default size of 256 x 256. These images are then converted to the grayscale image having entries numbered between, 0 to 255. As there will be chances of the noise induced in the image, causing reduction in the accuracy, also in the capacity of tumor segmentation if present by giving fault result, it is always preferable to use an efficient noise removal filter. In the proposed work we made use of Weiner filter. As this filter has the robustness to preserve the important feature like edge.

3.2 **Fuzzy based Image Fusion using RPCA and Quad tree Decomposition**

Entire frame work of this Fuzzy based image fusion is as shown in the Fig. 2. It is proven that the RPCA is to be one of the effective techniques to recover both spare and low rank components from the data of high dimension. In this approach a data input matrix $D \in i^{M \times N}$ is made to subject itself to low rank property. To regain the structure of low-rank, D can be decomposed as given below,

$$D = A + E, \qquad rank(A) = \min(M, N) \qquad (1)$$

Where principle matrix is represented by matrix A and spare matrix is represented by matrix E. Hence to overcome this difficult task a demonstration is done saying that w.r.t the rank of A and also when the spare matrix E is sufficiently spare, accurate recovery of the Matrix A from D is done only on solving the optimized problem given below,

$$\min_{(A,E)} \|A\|_* + \lambda \|E\|_1 \quad s.t. \quad A + E = D \qquad (2)$$

Where $\|\cdot\|_*$ depicts the nuclear norm of the principle matrix A, $\|\cdot\|_1$represents the l_1 norm of the spare matrix E and positive weighting parameter is denoted by λ.

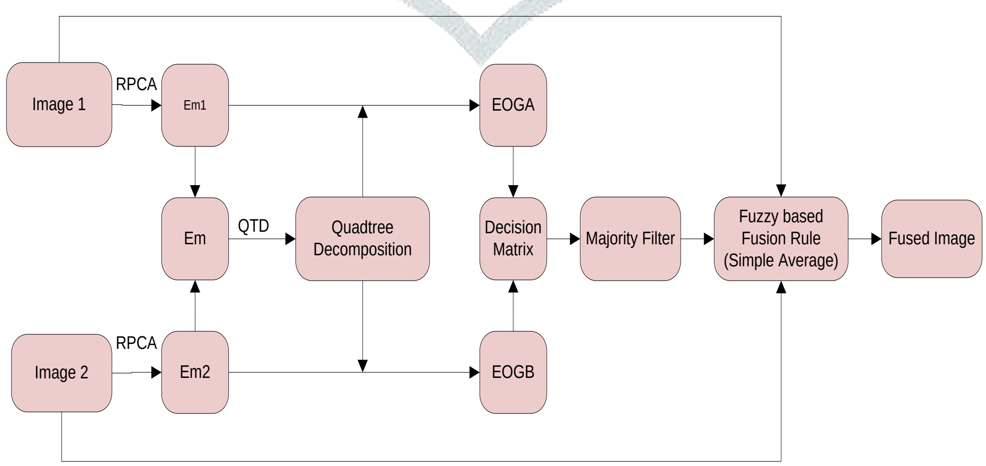

Fig. 2: Block Diagram for Fusion using RPCA and Quad Tree Decomposition

In the Quad Tree Decomposition (QT) structure, each one of these internal nodes has four partitions and these leaf nodes present in the tree has no partition. This analysis technique always partition image into blocks. These blocks are comparatively more homogeneous to the image itself. In the traditional technique of QT decomposition, a sized image is always divided into parts of four equal sized blocks and these blocks are checked with some threshold conditions of homogeneity regions. If the divided block reaches the threshold condition then it is not divided further, blocks which will not meet this criteria is divided further into four blocks. This step is continued till the blocks meet the threshold condition. Processing of this decomposition, division approach is first performed on the image with low resolution and then on the image with high resolution based on the low resolution image division. This approach is chosen for its self adaption and high speed property. This approach also eliminated artifacts involved in the fused image.

The proposed technique for fusion approach is as shown in the Fig. 2. The detailed steps for both these approaches are given in the flowchart given in the Fig. 3. In the proposed approach a novel method of fusion is carried out. An optimal approach of subdivision is obtained using an efficient QT decomposition technique. As in the flow given below, two source images Image 1 and Image 2 is taken and are presumed to be preregistered before passing as the input. Matrix D as explained above using RPCA decomposition approach is constructed. Once the decomposition is done principle matrix A and spare matrix E is obtained. Based on the salient homogeneity region of the matrix E the better partition of Matrix E always corresponds for the improved partition of the spare matrix. The temporary fusion spare matrix is constructed by averaging the two matrices. Next step is partitioning the temporary spare matrix into number of blocks using QT decomposition. Based on the results obtained to this matrix two spare matrices are split. As described above if the region homogeneity of the block does not meet the defined threshold conditions they are terminated for further QT decomposition. Next step is to calculate the sharpness as in the eq. (3) below, where E_{m1} and E_{m2} are the spare matrix blocks obtained. $E_{m1}^{(k)}$ And $E_{m2}^{(k)}$ denote the kth blocks of sparse matrices E_{m1} and E_{m2} respectively. $EOG_k^{E_A}$ Denotes the EOG-Energy of Image Gradient and $EOG_k^{E_B}$ be the EOG of $E_{m1}^{(k)}$ and $E_{m2}^{(k)}$, accordingly. EOG of each sparse matrix block can be defined as,

$$\begin{cases} EOG = \sum_i \sum_j (E_i^2 + E_j^2) \\ E_i = E(i+1, j) - E(i, j) \\ E_j = E(i, j+1) - E(i, j) \end{cases} \tag{3}$$

Where $E(i, j)$ represents the value of the element at the position (i, j) in sparse matrix block. Followed by creating decision matrix using the eq. (4) is done. Where “1” in H depicts the pixel at position (i, j) in the input Image 1 becomes clearer, and while “0” in H represents the pixel at position (i, j) in the input Image 2 becomes clearer [26]. Final fused image is obtained using the fusion rule given in the eq. (5).

$$H(i, j) = \begin{cases} 1, & EOG_k^{E_A} \geq EOG_k^{E_B} \\ 0, & \text{otherwise} \end{cases} \tag{4}$$

$$F(i, j) = \begin{cases} \text{Image1}(i, j), & H(i, j) = 1 \\ \text{Image2}(i, j), & H(i, j) = 0 \end{cases} \tag{5}$$

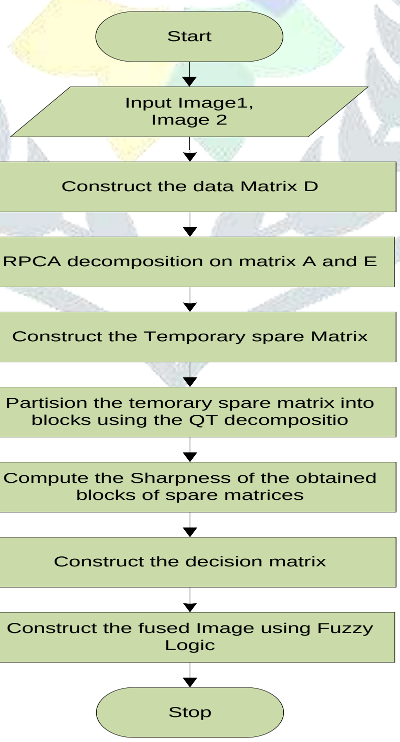

Fig. 3: Flowchart for Fusion Technique using RPCA and Quad tree Decomposition

Once the final fused image is obtained they are again compared with certain fuzzy rules. Usually fuzzy machines will always work on certain fuzzy sets for decision making to perform better fusion. The RPCA decomposition used in our research work is decomposing image with 6 iterations, for the image of dimensions 256 X 256, here the dimensions include number of row and column number. For the RPCA decomposition of two images T1 and T2 all the pixels are concatenated into one vector form of size 65536.

3.3 Level Set Segmentation

This segmentation approach is a kind of curve propagation based approach which is used in our project for segmentation. Curve propagation is one of the popular approaches, which is used in different applications like object tracking, object extraction and stereo reconstruction. Level set approach is one of the emerging image segmentation approaches for the segmentation of the medical images. This approach is important in tracking shapes and interfaces. The basic idea behind this approach is to represent contours as the level set of zero of an implicit function defined in high dimension, which is usually referred as level set function.

Level set segmentation method can be formulated with strong mathematical theories as follows, Initially starts with setting of segmentation boundaries in which the contour level must be at zero level, for this the implicit surface is given as,

$$\emptyset(X, t) = \mp d \qquad (6)$$

Where $\emptyset$ = Implicit Surface, X= Position of taken image, t = Time, d= Distance between X and the zero level set. 'd' values varies as positive or negative, the condition behind this is, if 'X' position is outside zero level set then 'd' is positive or else 'd' is negative [27].

By tracking and interfacing the level zero set $\tau(t)$ it will be very much easy to approximate the active contours evaluation which is directly dependent on PDE function$\emptyset(t, x, y)$. Implicit interface of zero level set is given by

$$\tau(t) = \begin{cases} \emptyset(t, x, y) < 0 & (x, y) \text{ is inside } \tau(t) \\ \emptyset(t, x, y) = 0 & (x, y) \quad \text{is at } \tau(t) \\ \emptyset(t, x, y) > 0 & (x, y) \text{is outside } \tau(t) \end{cases} \qquad (7)$$

By knowing the level set function values it is pretty much easy to estimate the topological changes of the implicit interface 'τ', numerical equation for level set with evolution of '$\emptyset$" is given by,

$$\begin{cases} \frac{\partial \emptyset}{\partial t} + F|\nabla \emptyset| = \quad 0 \\ \emptyset(0, x, y) = \emptyset_0(x, y) \end{cases} \qquad (8)$$

Where $|\nabla\emptyset|$= Normal directionType equation here.

$\emptyset_0(x, y)$= Contour at initial levels

F= Internal and external forces

By using the edge indication function 'h' the forces can be normalized in order to block the level set evolution along with the optimal solution,

$$h = \frac{1}{1 + |\nabla(G_\sigma * I)^2|} \qquad (9)$$

Where G_σ represents the Gaussian kernel and I is the considered image. Level set segmentation standard formula with all the parameters which are explained above is given as

$$\frac{\partial \emptyset}{\partial t} = h|\nabla\emptyset| \left(\mathrm{div} \left(\frac{\nabla \emptyset}{|\nabla \emptyset|} \right) + v \right) \qquad (10)$$

The computation time for all the steps and mathematical theories as very high in order to overcome these drawbacks and also to get better output the fuzzy clustering technique is combined with the level set segmentation technique to form one hybrid technique called spatial fuzzy clustering algorithm, which is explained in the previous section. For the proposed research work 256 X 256 dimensional passing of images to level set segmentation that segments image with iterations of 198.

3.4 Feature Extraction

A typical MRI image contains a large amount of heterogeneous information that depicts the different vessels, tissues and different other characteristics. In order to build an efficient diagnosis system towards correctly classifying the normal and the diseases regions present in the MRI image, presenting all the information which is available that is present in the image to the diagnosis system so that it can efficiently discriminate between normal and abnormal tissue. However the usage of all these heterogeneous information results to the high dimension feature vectors which will lead to the degrading of diagnostic accuracy and increase the computational complexity. Therefore considering the reliable feature vectors among them is very necessary to reduce the amount of irrelevant information hence producing efficient descriptors of the compact size. The measurements of one or more functions are called as features.

Quantifiable property of an object is specified by each of these features and only significant information's are later picked from these features. Features are classified into different types which are general features and global features. The features which are independent based on the application are called general features. The features which are obtained during the edge detection by considering the subdivision of the bands of the image and segmentation of the image are called as local features. The two features used in this work are Grey-Level Co-Occurrence Matrix (GLCM) and Grey-Level Run-Length Matrix (GLRLM). In our work 128 X 128 image dimension is passed to GLCM, this will calculate approximately 22 features for the query image. Total features calculated by GLCM are 1 X 44 vectors. Similarly GLRLM is generating features of number 7 i.e.1 X 7 vector. So the total number of features developed by both techniques is 1 X 51 vectors.

*3.4.1 **Grey-Level Co-Occurrence Matrix***

In a statistical analysis of texture, on the basis of statistical distribution of pixel, computation of the texture features at a given position relative to others in a matrix consisting of pixels representing the image. Depending on the pixel number in each of the combination, first order statistics, second order statistics or higher order statistics are considered. Based on the GLCM the second order statistics is used to analyze the image as a texture. GLCM approach is the tabulation of the frequency or how often a combo of pixel brightness values in an image is occurred. The Fig. 4 given below represents the GLCM formulation of the grey level of four levels in an image of distance d = 1 and the 0° direction.

Fig. 4 (a) depicts the example matrix of the pixel intensity which represents the image with four levels of grey. The intensity level 1 and 0 are marked within a thin box. The thin box represents the pixel intensity 0 with the pixel intensity 1 as its neighbor. There are usually two occurrences of pixels of such types. Hence the matrix of GLCM is formed as in Fig. 4 (b) with value two in 0 rows, column 1. Similarly GLCM matrix column

0 and row 0 is also has been given a value of two, because of occurrences of two in which the pixel with the value 0 has 0 pixel as its neighbor in the horizontal direction. Due to which the pixels matrix in (a) can be transformed into a GLCM as (b). Not only to the horizontal direction, GLCM can also be formed for different directions like 90 º, 45 ºand 135 º as depicted i the Fig. 5 [28].

0	0	1	1	1
0	0	1	1	1
0	2	2	2	2
2	2	3	3	3
2	2	3	3	3

(a)

	0	1	2	3
0	2	2	1	0
1	0	4	0	0
2	0	0	5	2
3	0	0	0	4

(b)

Fig. 4: (a) Example Matrix of the Pixel Intensity; (b) GLCM Matrix

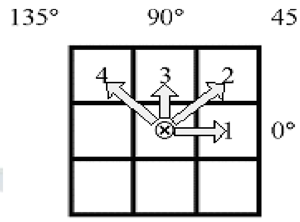

Fig. 5: Different Directions Formed by GLCM

From centre to the 1st pixel representing direction = 0° with distance d =1, to the pixel 2 direction = 45° with the distance d = 1 and also to the 3rd pixel direction = 90° with distance d = 1, and to the pixel 4 direction = 135° with distance d = 1. Even though the co-occurrence matrices extract the properties of texture, it is not directly used an analysis tool. The matrix of this is again extracted to fetch the numbers that is usually used for texture classification. The above created GLCM matrix is then applied to segmented regions. Mathematically, for a given image I of size $K \times K$ (256×256), the elements of a $G \times G$ $(8 \times 8 \times 4)$ gray-level co-occurrence matrix MCO for a displacement vector $d = (dx, dy)$ is defined as in eq. (11). The defined value d for angle 0 is [0 d], for angle 45 is [-d d], angle for 90 is [-d 0] and for degree 135 is [-d d].

$$M_{co} = \sum_{x=1}^{k}\sum_{y=1}^{k}\begin{cases}1, \text{if } I(x,y) = i \text{ and } I(x+d_x, y+d_y) = j \\ 0\end{cases} \quad (11)$$

In the proposed work four important features like contrast, energy, entropy and Correlation are extracted. Contrast calculates the intensity level difference between the adjacent pixels in an considered image and is given as fallows by the equation below,

$$\text{Contrast} = \sum\nolimits_{i,j} |i-j|^2 p(i,j) \quad (12)$$

Where $p(i, j)$ denotes the position of the GLCM in that the value represents the sum of co-occurrence between adjacent pixels of i and its neighbor j. Correlation measures the level of correlations between pixels against the remaining pixels in the Input image. Also Correlation computation finds the linear dependency levels of grey of the neighboring pixels and is it is given by,

$$\text{Correlation} = \sum\nolimits_{i,j} \frac{(i-\mu_i)(j-\mu_j)p(i,j)}{\sigma_i \sigma_j} \quad (13)$$

Energy measure the summation of squared element in the entire GLCM. It is denoted by the eq. (15),

$\text{Energy} = \sum_{i,j} p(i,j)^2$ (14)

Information which compress the considered image and it contains the loss of information from the image for GLCM calculation is referred as entropy and it is given as,

$$\text{Entropy} = \sum_{i=0}^{N_g-1}\sum_{j=0}^{N_g-1} -p_{ij} * \log p_{ij} \quad (15)$$

The formulation and extraction of the input NPK segments are extracted using MATLAB for calculating GLCM to get feature vector.

3.4.2 ***Gray-Level Run-Length Matrix (GLRLM)***

GLRLM is nothing but a matrix from which the texture features is extracted for the analysis of texture. Usually this texture is called as the grey intensity pixel of pattern in a particular direction from the reference pixel. Run Length is defined as the pixel number that is adjacent having the same intensity of grey in the particular direction.

1	2	3	4
1	3	4	4
3	2	2	2
4	1	4	1

(b)

Gray Level	Run Length(j)			
	1	2	3	4
1	4	0	0	0
2	1	0	1	0
3	3	0	0	0
4	3	1	0	0

(b)

Fig. 6: (a) Matrix with 4 Different Gray Levels; (b) Values for Run Length

GLRLM is usually a two dimensional matrix, where each of the element $p(i, j|\theta)$ is the number of elements j with the intensity value i present in the directionθ. Fig. 5 depicts the matrix with 4 different gray levels.

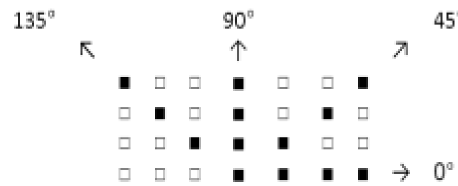

Fig. 7: Directions of GLRLM Matrix

These matrices represent the GLRL matrix in the direction 0° ($p(i, j|\theta)$, In addition with the 0°, GLRLM matrix can also be represented in the other direction i.e. 90 º, 45 ºand 135 º as depicted in the Fig. 7.

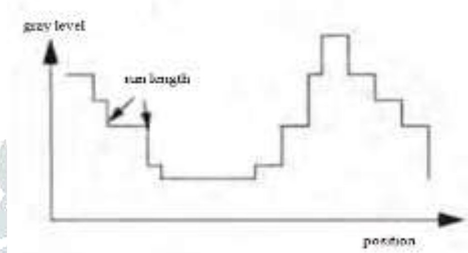

Fig. 8: Run Length of GLRLM.

Some of the texture features extracted from GLRLM are: SRE (Shot Runs Emphasis), GLN (Gray Level Non-uniformity), LRE (Long Run Emphasis), RP (Run Percentage) and RLN (Run Length Non-uniformity). Fig. 8 depicts the Run Length of GLRLM [27].

3.5 Back Propagation Neural Network (BPNN)

The general introductions for artificial neural network are explained briefly in this section. The proofs for existence of massive networks of neurons are given by the human brains. Acts like recognition of the faces, speech and activities like body movement and body function are computationally demanded by brain. Human brain is consisting of more than ten billion interconnected neurons. Each of this neuron is nothing but cell that usually uses biochemical reactions to transmit and receive information. As in Fig. 10 the tree like structure of networks of the nerve fibers are called as dendrites and they are connected to cell body (Soma), is the location where neurons are presented. Single and long fiber is called axon is extended from body of the cell which will eventually branches into substrands and strands, that are connected to other neurons through a terminal called synaptic or synapses. The process in which from the sending end of the junction the specific substances of the transmitter substances are all released in a complex chemical process.

Transmission of signals in synapses from one of the neuron is done to generate these chemical processes. To lower or raise electrical potential within body of the receiving cell this effect is utilized. The cell is fired if the potential exceeds the threshold. Here the ANN (Artificial neural networks) is as developed as generalizations for the mathematical items of the biological nervous systems. The basic elements of the processing elements of neural networks are neurons or it may be artificial neurons or nodes. In the mathematical model of neural the modulation of the associated input signals are done by the connection weights which represents synapses. Transfer function represents the nonlinear characteristics exhibited by neurons. The detailed architecture of neural network is explained briefly below [29], [30].

Classifier will initiate the classification by defining architecture for network. This includes the neurons network number and layers in the network. Once based on the collected features network is created it intakes the features for training Data. The trained features are compared with the current features of query image. If the satisfactory level is achieved for the particular feature output layer is updated if not then loop will be continued until the query image are matched with any one section of trained data. Fig. 9 gives the flow of ANN.

ANN architecture mainly consists of 3 types of the neuron layers called input layer, hidden and output layer. In feed forward kind of networks signal flow is mainly from the input to output units. Exactly in the feed forward direction. The processing of data can extended over multiple layers of units with the absence of feedback connections. Feedback connections are present in recurrent networks. A neural network should be configured in such a way that system with the input set produces the desired set of the outputs. To set the connection strengths various methods exists

Using the prior knowledge weights is set explicitly. Another approach is to train the network by feeding it with teaching pattern and according to few learning rules letting it to change its weights. There are 3 different sorts of learning situations: reinforcement learning, Supervised and non supervised learning. In the supervised learning approach input vector along with desired responses are represented at the input. Forward pass and the error calculation between the actual and desired response are also done. In the supervised learning approach desired signals on individual output nodes are given by an external teacher.

- Perceptron Learning

The perceptron is another form of neural network in which the weights and the bias are trained to produce a correct target vector. The Technique used here for learning is called perceptron learning. Perceptrons are suited for simple problems in pattern classification.

- Back propagation Learning

Only linearity independent problems or linearity separable problems are handled by simple perceptron. With respect to each weight by taking partial derivative of network error, here we will learn little about error direction moving in the network. The rate change of the error has the value of the weights i.e. if we take the negative of the derivative then proceeding to add it to the weights make the error decrease until it reaches local minima. This tells us that the error is increasing when the weight is increasing. And hence adding negative value to the weight is an obvious thing and vice versa if in case of negative derivative. When you consider that the taking of those partial derivatives after which applying them to every of the weights takes position, establishing from the output layer to hidden layer weights, then the hidden layer to input layer weights because it turns out, that is integral on the grounds that changing these set of weights requires that we all know the partial derivatives calculated within the layer downstream, this algorithm has been known as the back propagation algorithm. Two different modes of neural network training are followed: batch and online mode.

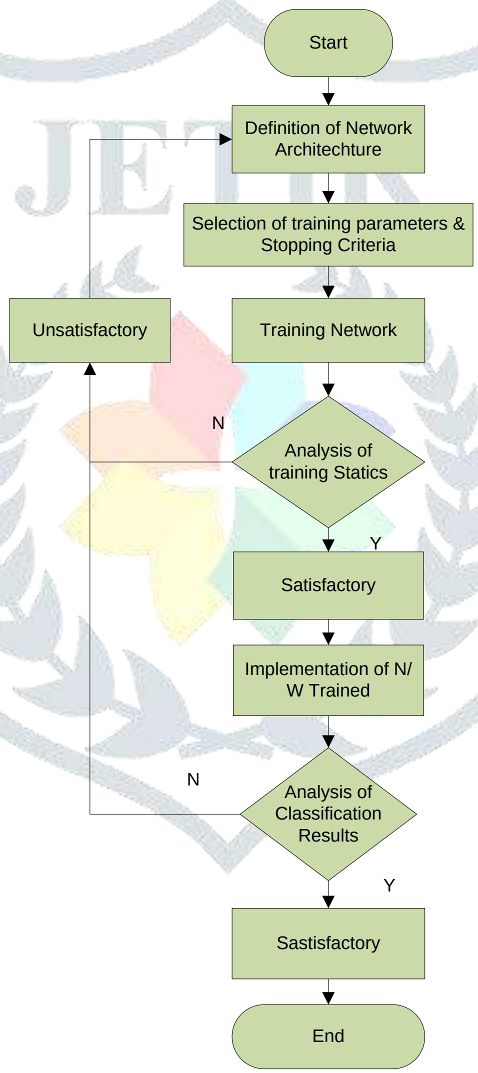

Fig. 9: ANN Training Module Flow Chart

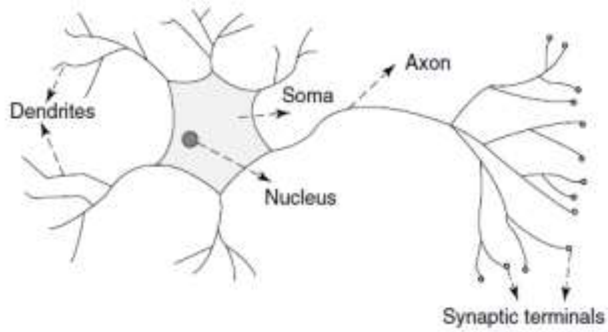

Fig. 10: Treelike Networks of the Nerve Fibers in ANN

Algorithm 1: Back Propagation Neural Network

Input: weights of segmented Image
Output: classified tumor section
Step1: Choose initial weights randomly w_i
Step2: While Error is too large
Step3: For loop Consider training pattern present in the random order
Step4: Apply the inputs
Step5: For every neuron η calculate output pattern O_p in output layer from input layer, through hidden layer.
Step6: At output layer calculate error.

$$O_{\eta p}\,(\text{Network}) = \frac{1}{1 + e^{-\lambda \text{network}_\eta}}$$

Here, network_η is connection of weights from input k to neurons η

$$\text{network}_\eta = \text{bias} * w_{\text{bias}} + \sum_k O_{pk}\, w_{k\eta}$$

Step7: pass the error $O_{\eta p}$ (Network) to compute errors for pre-output layer.
Step8: Compute weights using error.
Step9: Apply the weights.
Step10: If Training pattern is < 1
End for
End

The number of weight updates of the two approaches for the equal number of information shows it is very difficult. The online process weight updates are computed for each and every input data pattern and the weights are modified after each sample. A replacement answer is to compute the weight replaces for each and every input sample, but store these values during one pass by means of the training set which is referred to as an epoch.

At the epoch end, addition of all of the contributions, and weights might be made up to date with the composite value. This process adapts the weights with a cumulative update it is known as the batch-training mode. Training involves feeding the training samples as input vectors through a neural network, error calculation of the output layer and weight adjustment to minimize error in the network. In the research work we are making use of 51 neurons at input layer, 25 neurons at hidden layer and 3 neurons at output layer.

IV. Experimental Result

Experiments were conducted on MATLAB R2012a. The collected dataset of 166 MRI images where calcified into tumor and non tumor to train the algorithms and to evaluate the classification and also tumor identification accuracy by cross validation with the ground truth. For each of the MRI images 51 features extracted using GLCM and GLRLM methods. This section depicts the overall results obtained at each stage of the proposed system. Initially the query inputs T1 and T2 slice of the input MRI images as in Fig. 11(a) and (b) is taken and pre-processed to get the noise removed image as in (c) and (d). Next step is to get fused image using techniques like RPCA and QT decomposition to get the fused image as in (e). Once the fused image is obtained it is necessary for us to predict the exact tumor region. For proper prediction segmentation of the tumor becomes very important. Segmentation is done using the Level set Algorithm.

Level set algorithms undergo 198 iterations to find the tumor regions as in (f) and give the final output as in (g). Output of this stage is then compared with the threshold values to detect the tumor regions as in (h). These segmented regions may be tumor or non tumor, hence to detect the exact tumor feature extraction is done using the techniques like GLCM and GLRLM and is passed to ANN classifier to classify whether it is tumor or non tumor region. The tumor area after classification is as shown in the (i). The validated tumor region is then located in the fused image as in (j). The algorithm is evaluated on different MRI images consisting of tumor regions. Experiments say that the proposed systems give good results when compared to the existing systems.

Fig. 12 (a) and (b) depicts the input image T1 and T2. These images undergo pre-processing steps to get the noise removed images to make it fit for the next stages. These images are later fused to get the fused image. Segmentation of tumor regions in this fused image is done using the level set algorithms. These segments may be tumor or non tumor; hence the validation on this is done using ANN classifier as in (d). The detected tumor is then located in the fused image as in (d). Similarly Fig. 13 (a) depicts the Input T1 Image and (b) depicts the Input T2 Image, (c) gives the segmented tumor parts obtained and (d) gives the validated tumor part after classification and (e) depicts the detected tumor location in the fused image.

Similarly Fig. 14 (a) depicts the Input T1 Image and (b) depicts the Input T2 Image, (c) gives the Segmented Tumor Parts obtained and (d) gives the Validated Tumor Part after classification and (e) depicts the Detected tumor Location in the Fused Image.

$$\text{Precision} = \frac{TP}{TP + FP} \tag{16}$$

$$\text{Recall} = \frac{TP}{TP + FN} \tag{17}$$

$$\text{Accuracy} = \frac{TP + TN}{TP + FP + TN + FN} \tag{18}$$

$$\text{Sensitivity} = \frac{TP}{TP + FN} \tag{19}$$

$$\text{Specificity} = \frac{TN}{FP+TN} \tag{20}$$

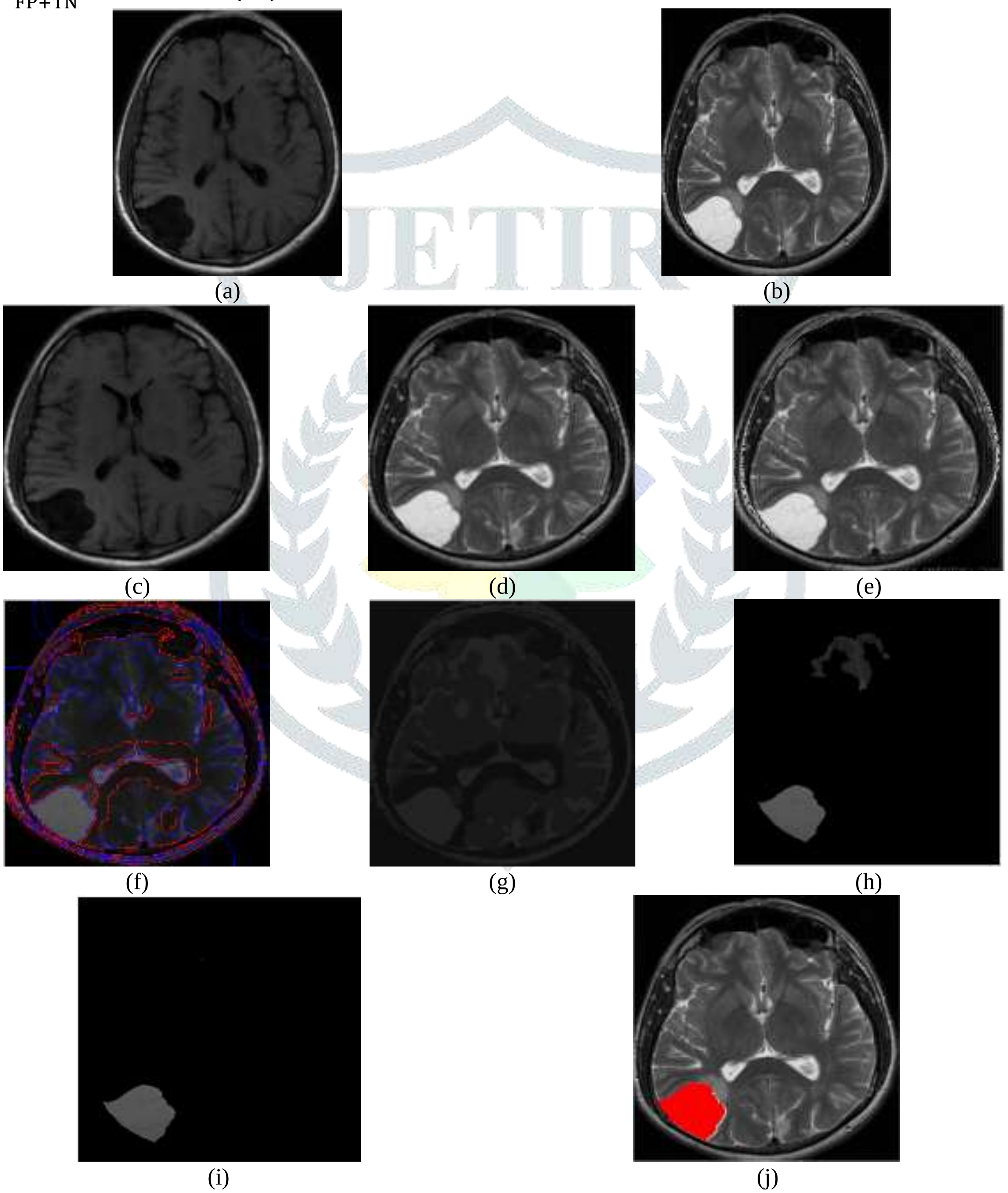

Fig. 11: (a) Input T1 Image; (b) Input T2 Image; (c) Filtered T1 Image; (d) Filtered T2 Image; (e)198 Iterations in the Fused Image; (f) Level Set Segmented Image; (g) Segmented Tumor Parts; (h) Validated Tumor Part; (i) Detected tumor Location in the Fused Image.

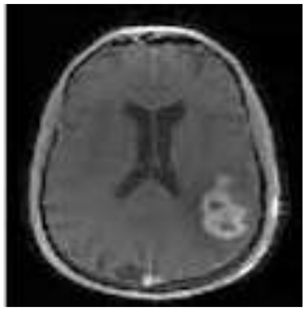
(a)

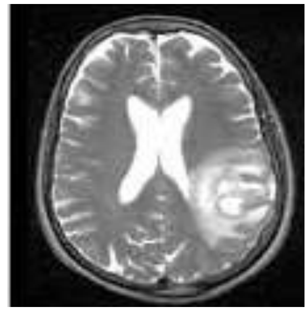
(b)

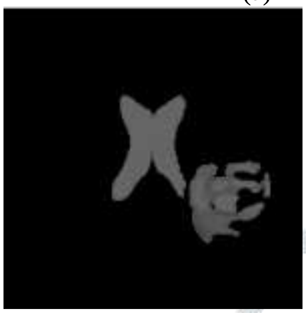
(c)

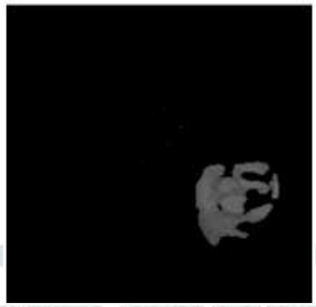
(d)

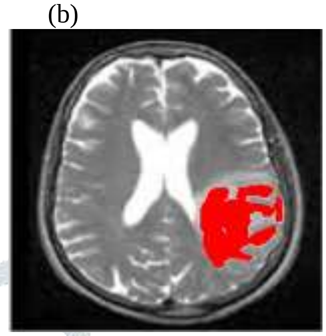
(e)

Fig. 12: (a) Input T1 Image; (b) Input T2 Image; (c) Segmented Tumor Parts; (d) Validated Tumor Part; (e) Detected tumor Location in the Fused Image.

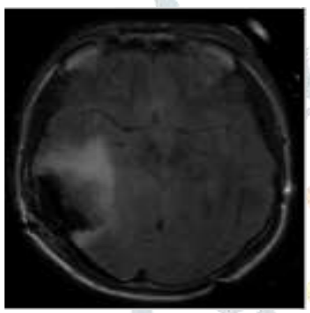
(a)

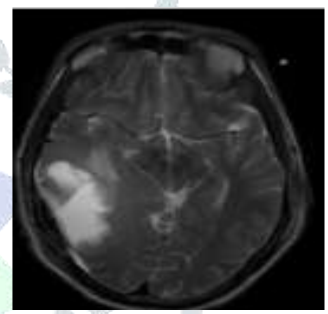
(b)

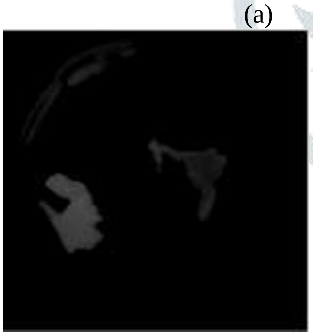
(c)


(d)

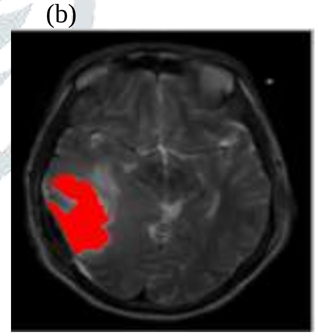
(e)

Fig. 13: (a) Input T1 Image; (b) Input T2 Image; (c) Segmented Tumor Parts; (d) Validated Tumor Part; (e) Detected tumor Location in the Fused Image.

Fig. 14: (a) Input T1 Image; (b) Input T2 Image; (c) Segmented Tumor Parts; (d) Validated Tumor Part; (e) Detected tumor Location in the Fused Image.

sTable 1: Confusion Matrix

N = 166	Predicted No	Predicted Yes	
NO	TN = 52	FP = 5	**57**
Yes	FN = 5	TP = 104	**109**
	57	**109**	

Table 3, 4, 5 and 6 depicts the comparison table for the proposed systems and the existing systems in terms of accuracy, recall, sensitivity and specificity and it is found that that proposed system gives good results when compared to the existing systems. Similarly Fig. 16 depicts the graph for the proposed system and Fig. 17 depicts the comparison results obtained for the proposed system when compared with the ground truth values. Ground truth values are the results obtained after manual calculation of tumor sections in the medical image or dataset. The number of white pixels available in the tumor sectors is calculated manually and this number is compared with pixels available at classified tumor section by the proposed system. Less the difference between the parameter, better the segmentation; can be concluded with ground truth value. Our proposed method is almost lying nearer to the ground truth value as shown in Fig. 17.

Table 2: Performance Analysis Table for the Proposed System

Dataset	Accuracy	Precision	Recall	Sensitivity	Specificity
1 (34 images)	94.11	95.45	95.45	95.45	91.66
2 (34 images)	94.11	95	95	95	92.85
3 (30 images)	93.33	95.23	95.23	95.23	95.23
4 (36 images)	94.44	95.83	95.83	95.83	95.83
5 (32 images)	93.75	95.45	95.45	95.45	95.45
Average (166 images)	93.95	95.39	95.39	95.39	94.20

Fig. 15: (a), (b), (c), (d), (e) are the Performance analysis graph for Proposed System

Table 3: Comparison Table for Proposed and Existing Systems for Accuracy.

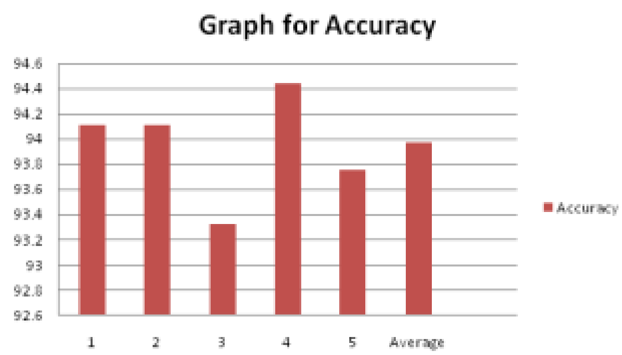

(a)

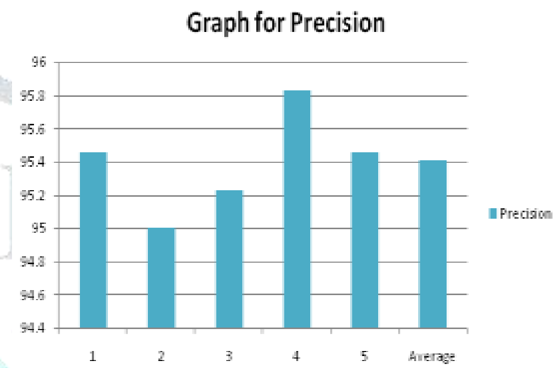

(b)

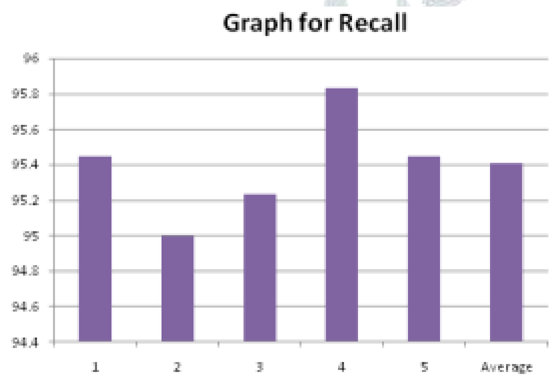

(c)

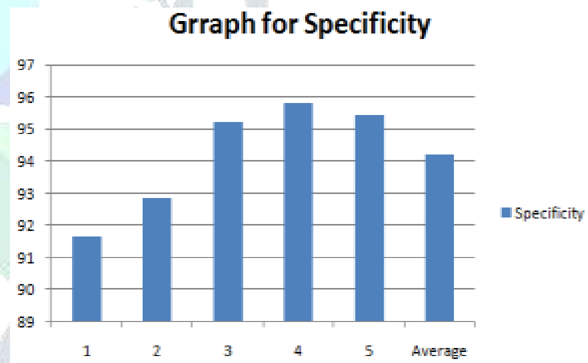

(d)

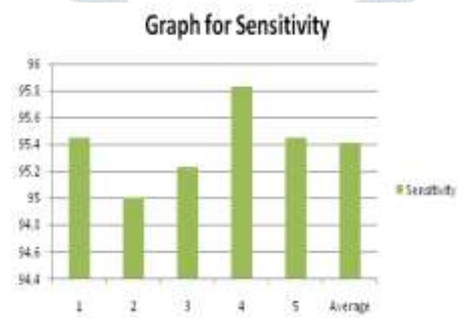

(e)

Reference	Methods	Accuracy
An Automatic Brain Tumor Extraction System Using Different Segmentation [31]	Otsu + K-means + Fuzzy-C-Means + Thresholding algorithm	90.57
Analysis of the Brain MRI for Tumor detection & Segmentation [32]	Otsu's segmentation + Overlay based image fusion	93.00

Brain tumor segmentation based on a hybrid clustering technique [33]	K-means Clustering + Fuzzy-C-Means	90.50
Analysis And Evaluation Of Brain Tumor Detection From MRI Using F-PSO And FB-K Means [14]	Fuzzy bisector K-means + Fractional PSO based neural network	78.00
Brain tumors detection and segmentation in MR images: Gabor wavelet vs. statistical features [09]	PCA with statistical features	79.30
Proposed	RPCA and Quad tree Decomposition based fusion + GLCM + GLRLM+ ANN	96.95

Table 4: Comparison Table for Proposed and Existing Systems for Recall.

Reference	Methods	Recall
Brain tumor segmentation based on a hybrid clustering technique [33].	Otsu + K-means + Fuzzy-C-Means + Thresholding algorithm	90.5
Analysis And Evaluation Of Brain Tumor Detection From MRI Using F-PSO And FB-K Means[14]	Fuzzy bisector K-means + Fractional PSO based neural network	77
Brain Tumor Segmentation with Deep Neural Networks [34]	Subsequent ANN	84
Brain tumors detection and segmentation in MR images: Gabor wavelet vs. statistical features [09]	PCA with statistical features	77.2
Proposed	RPCA and Quad tree Decomposition based fusion + GLCM + GLRLM+ ANN	95.41

Table 5: Comparison Table for Proposed and Existing Systems for Specificity.

Reference	Methods	Specificity
Analysis And Evaluation Of Brain Tumor Detection From MRI Using F-PSO And FB-K Means [14]	Fuzzy bisector K-means + Fractional PSO based neural network	80
Brain Tumor Segmentation with Deep Neural Networks [34]	Subsequent ANN	88
Brain tumors detection and segmentation in MR images: Gabor wavelet vs. statistical features [09]	PCA with statistical features	81.3
Proposed	RPCA and Quad tree Decomposition based fusion + GLCM + GLRLM+ ANN	91.22

Table 6: Comparison Table for Proposed and Existing Systems for Sensitivity.

Reference	Methods	Sensitivity
Brain tumor segmentation based on a hybrid clustering technique [33]	Otsu + K-means + Fuzzy-C-Means + Thresholding algorithm	90.5
Analysis And Evaluation Of Brain Tumor Detection From MRI Using F-PSO And FB-K Means [14]	Fuzzy bisector K-means + Fractional PSO based neural network	77
Brain Tumor Segmentation with Deep Neural Networks [34]	Subsequent ANN	84
Brain tumors detection and segmentation in MR images: Gabor wavelet vs. statistical features [09]	PCA with statistical features	77.2
Proposed	RPCA and Quad tree Decomposition based fusion + GLCM + GLRLM+A NN	95.41

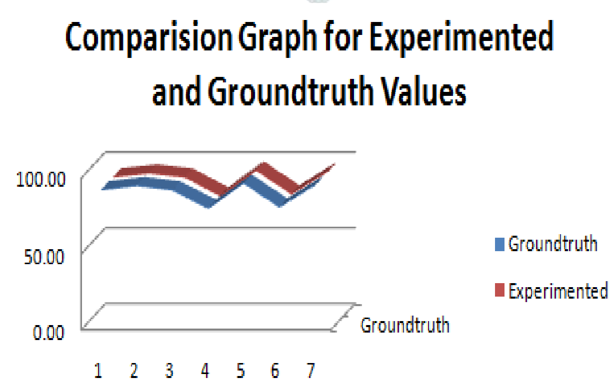

Fig. 17: Comparison Graph for Proposed and Ground Truth Values

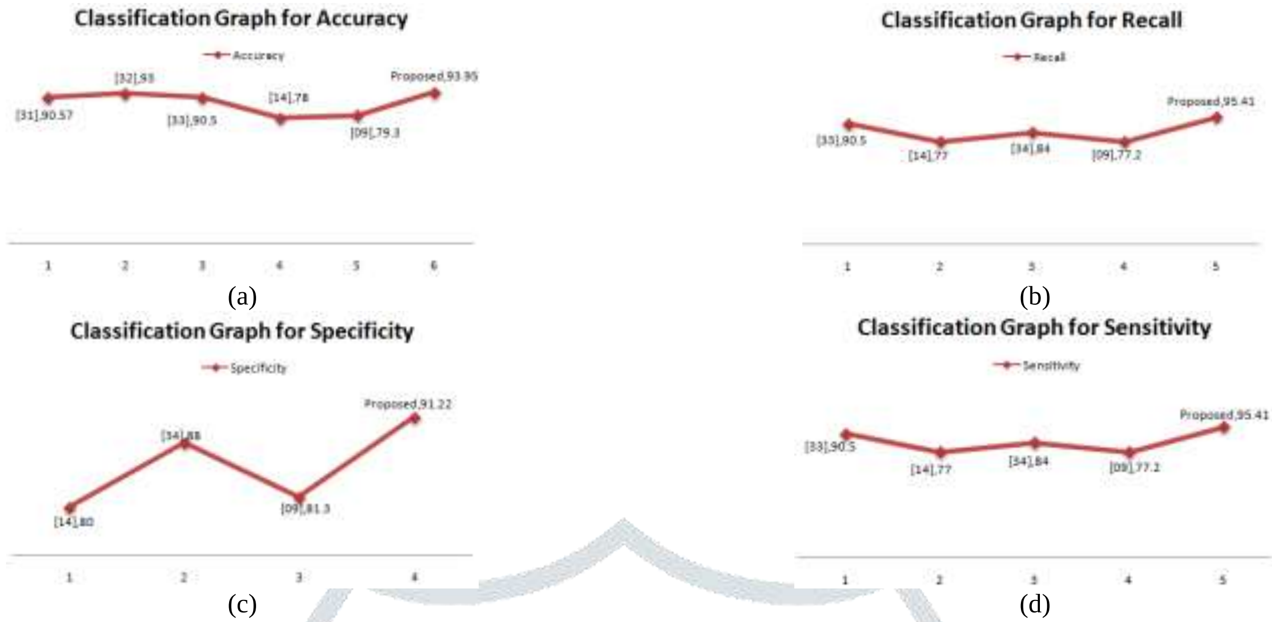

Fig. 16: Comparison Graph for Proposed and Existing Systems.

V. Conclusion

Abnormal and uncontrolled growing of cells inside the brains leads to brain tumor. Usually treatment of these brain tumors depends on location and size of tumor. Although benign tumors do not tend to spread, but they may cause severe damage to brain by pressing its areas if not treated in early stage. Hence to avoid the manual errors an efficient automated intelligent classification technique is proposed. This work also involves an efficient fusion technique to fuse T1 and T2 MRI slices of brain, robust method like level set segmentation is also used to segment the tumor region, feature extraction methods like GLRLM and GLCM to extract features and ANN classifier for efficient detection and classification of the brain tumor. The algorithm is evaluated on different MRI brain tumor images to get an efficient tumor detection system with good performance when compared to the existing systems.

Reference

[1] Mohammad Havaei, Axel Davy, David Warde-Farley, Antoine Biard, Aaron Courville, Yoshua Bengio, Chris Pal, Pierre-Marc Jodoin and Hugo Larochelle, "Brain Tumour Segmentation with Deep Neural Networks", 2016.

[2] Bjoern H. Menze, Andras Jakab, Stefan Bauer, Jayashree Kalpathy-Cramer, Keyvan Farahani, Justin Kirby, Yuliya Burren, Nicole Porz, Johannes Slotboom, Roland Wiest, Levente Lanczi, Elizabeth Gerstner, Marc-André Weber, Tal Arbel, Brian B. Avants, Nicholas Ayache, Patricia Buendia, D. Louis Collins, Nicolas Cordier, Jason J. Corso, Antonio Criminisi, Tilak Das, Hervé Delingette, Çağatay Demiralp, Christopher R. Durst, Michel Dojat, Senan Doyle, Joana Festa, Florence Forbes, Ezequiel Geremia, Ben Glocker, Polina Golland, Xiaotao Guo, Andac Hamamci, Khan M. Iftekharuddin, Raj Jena, Nigel M. John, Ender Konukoglu, Danial Lashkari, José António Mariz, Raphael Meier, Sérgio Pereira, Doina Precup, Stephen J. Price, Tammy Riklin Raviv, Syed M. S. Reza, Michael Ryan, Duygu Sarikaya, Lawrence Schwartz, Hoo-Chang Shin, Jamie Shotton, Carlos A. Silva, Nuno Sousa, Nagesh K. Subbanna, Gabor Szekely, Thomas J. Taylor, Owen M. Thomas, Nicholas J. Tustison, Gozde Unal, Flor Vasseur, Max Wintermark, Dong Hye Ye, Liang Zhao, Binsheng Zhao, Darko Zikic, Marcel Prastawa, Mauricio Reyes and Koen Van Leemput, "The Multimodal Brain Tumour Image Segmentation Benchmark (BRATS)", IEEE, Vol. 34, Issue 10, 2015.

[3] Nelly Gordillo, Eduard Montseny and Pilar Sobrevilla, "State of the art Survey on MRI Brain Tumour Segmentation", Elsevier, Vol. 31, Issue 8, pp. 1426-1438, 2013.

[4] Xavier Llado, Arnau Oliver, Mariano Cabezas, Jordi Freixenet, Joan C. Vilanova, Ana Quiles, Laia Valls, Lluis Ramio-Torrenta and Àlex Rovira, " Segmentation of Multiple Sclerosis Lesions in Brain MRI: A Review of Automated Approaches", Elsevier, Vol. 186, pp. 164 – 185, 2012.

[5] M.H. Fazel Zarandi, M. Zarinbal and M. Izadi, "Systematic Image Processing for Diagnosing Brain Tumour S: A Type-II Fuzzy Expert System Approach", Elsevier, Vol. 11, 285–294, 2011.

[6] El-Sayed Ahmed El-Dahshan, Tamer Hosny and Abdel-Badeeh M. Salem, "Hybrid Intelligent Techniques for MRI Brain Images Classification", Elsevier, Vol. 20, pp. 433 – 441, 2010.

[7] T. Logeswari and M. Karnan, "An Improved Implementation of Brain Tumour Detection Using Segmentation Based on Hierarchical Self Organizing Map", International Journal of Computer Theory and Engineering, Vol. 2, No. 4, 2010.

[8] Kailash Sinha and G.R.Sinha, "Efficient Segmentation Methods for Tumour Detection in MRI Images", IEEE, pp. 1 – 6, 2014.

[9] Nooshin Nabizadeh and Miroslav Kubat, "Brain Tumour Detection and Segmentation in MR Images: Gabor Wavelet vs. Statistical Features", Elsevier, Vol. 45, pp. 286 – 301, 2015.

[10] Manavalan Radhakrishnan and Thangavel Kuttiannan, "Comparative Analysis of Feature Extraction Methods for the Classification of Prostate Cancer from TRUS Medical Images", IJCSI International Journal of Computer Science Issues, Vol. 9, Issue 1, Issue 2, 2012.

[11] Anam Mustaqeem, Ali Javed and Tehseen Fatima, "An Efficient Brain Tumour Detection Algorithm Using Watershed & Thresholding Based Segmentation", I.J. Image, Graphics and Signal Processing, Vol. 10, pp. 34 - 39, 2012.

[12] Wright, John, Yigang Peng, Yi Ma, Arvind Ganesh and Shankar Rao, "Robust Principal Component Analysis: Exact Recovery of Corrupted Low-Rank Matrices via Convex Optimization", Advances in Neural Information Processing Systems, 2009.

[13] Trinadh babu and Sk.Salma begum, “An Adaptive MRI Tumour Detection Using Neural Network Based Adaboost Algorithm”, International Journal of Computer Science and Information Technologies, Vol. 6, Issue 1, pp. 42 - 47, 2015.

[14] Sheela.V.K and Dr. S. Suresh Babu, “Analysis and Evaluation of Brain Tumour Detection from MRI Using F-PSO and FB-K Means”, International Journal of Computer Science and Information Technology & Security (IJCSITS), Vol. 6, Issue 1, 2016.

[15] Mahantesh K and Kanyakumari, “BraTS: Brain Tumour Segmentation – Some Contemporary Approaches”, International Journal of Innovative Research in Science, Vol. 5, Issue 10, 2016.

[16] Fazli Wahid, Muhammad Fayaz and Abdul Salam Shah, “ An Evaluation of Automated Tumour Detection Techniques of Brain Magnetic Resonance Imaging (MRI)”, International Journal of Bio-Science and Bio-Technology Vol. 8, Issue 2, pp. 265 – 278, 2016.

[17] Dr.A.R. Kavitha, L.Chitra and R.kanaga, “Brain Tumour Segmentation using Genetic Algorithm with SVM Classifier”, International Journal of Advanced Research in Electrical, Electronics and Instrumentation Engineering, Vol. 5, Issue 3, 2016.

[18] Archana A.Mali and Prof.S.R.Pawar, “Detection & Classification of Brain Tumour”, International Journal of Innovative Research in Computer and Communication Engineering, Vol. 4, Issue 1, 2016.

[19] Samriti and Mr. Paramveer Singh, “Brain Tumour Detection Using Image Segmentation”, International Journal of Engineering Development and Research, Vol. 4, Issue 2, 2016.

[20] P.Senthil MA, “Image Mining Brain Tumour Detection using Tad Plane Volume Rendering from MRI (IBITA)”, JOC, Vol. 1 Issue 1, pp. 1 - 13, 2016.

[21] G. Venkateswara Rao and O. Koteswara Rao, “ Brain Tumour Detection and its Severity Analysis using Texture Features and Artificial Neural Network”, International Journal of Advance Research in Computer Science and Management Studies, Vol. 4, Issue 5, pp. 174 – 182, 2016.

[22] Irfan Mehmood, Naveed Ejaz, Muhammad Sajjad and Sung Wook Baik, “Prioritization of Brain MRI Volumes using Medical Image Perception Model and Tumour Region Segmentation”, Elsevier, Vol. 3, pp. 1471 – 1483, 2013.

[23] Leonardo Pacea, Emanuele Nicolaib, Angelo Luongoc, Marco Aiello, Onofrio A. Catalanob, Andrea Soricelli and Marco Salvatorec, “Comparison of Whole-Body PET/CT and PET/MRI in Breast Cancer Patients: Lesion Detection and Quantization of 18F-Deoxyglucose Uptake in Lesions and in Normal Organ Tissues”, Elsevier, Vol. 83 pp. 289– 296, 2014.

[24] Khan M. Iftekharuddin, Jing Zheng, Mohammad A. Islam and Robert J. Ogg, “Fractal-Based Brain Tumour Detection in Multimodal MRI”, Elsevier, Vol. 207, Issue 1, pp. 23 – 41, 2009.

[25] B. Hakyemez, C. Erdogan, G. Gokalp and A. Dusak, M. Parlak, “Solitary Metastases and High-Grade Gliomas: Radiological Differentiation by Morphometric Analysis and Perfusion-Weighted MRI”, Elsevier, Vol. 65, pp. 15 – 20, 2010.

[26] Yongxin Zhang, Li Chen, Zhihua Zhao and Jian Jia, “Multi-focus Image Fusion Based on Sparse Features”, International Journal of Signal Processing, Image Processing and Pattern Recognition Vol.7, Issue 2, pp. 399 – 410, 2014.

[27] Bing Nan Li, Chee Kong Chui, Stephen Chang and S.H. Ong, “Integrating Spatial Fuzzy Clustering with Level Set Methods for Automated Medical Image Segmenattion”, Springer, Vol. 41, pp. 1- 10, 2011.

[28] Aswini Kumar Mohanty, Swapnasikta Beberta and Saroj Kumar Lenka, “Classifying Benign and Malignant Mass using GLCM and GLRLM Based Texture Features from Mammogram”, International Journal of Engineering Research and Applications (IJERA), Vol. 1, Issue 3, pp. 687 - 693, 2011.

[29] Eltaher Mohamed Hussein and Dalia Mahmoud Adam Mahmoud, “Brain Tumour Detection using Artificial Neural Networks”, Journal of Science and Technology, Vol. 13, No. 2, 2012.

[30] N. Periyasamy and Dr. J. G. R. Sathiaseelan, “Detection and Classification of Brain Tumour Images Using Back Propagation Fuzzy Neural Network”, International Journal for Research in Applied Science & Engineering Technology (IJRASET), Vol. 3, Issue VIII, 2015.

[31] Arashdeep Kaur , “An Automatic Brain Tumour Extraction System Using Different Segmentation Methods”, IEEE, 2016.

[32] Imran Ahmed, Qazi Nida-Ur-Rehman, Ghulam Masood and Muhammad Nawaz, “Analysis of the Brain MRI for Tumour Detection & Segmentation”, Proceedings of the World Congress on Engineering, Vol. I, 2016.

[33] Eman Abdel-Maksoud, Mohammed Elmogy and Rashid Al-Awadi, “Brain tumor segmentation based on a hybrid clustering technique”, Egyptian Informatics Journal Vol. 16, pp. 71 – 81, 2015.

[34] Mohammad Havaeia, Axel Davyb, David Warde-Farleyc, Antoine Biardc,d, Aaron Courvillec, Yoshua Bengioc, Chris Palc,e, Pierre-Marc Jodoina and Hugo Larochellea, “Brain Tumor Segmentation with Deep Neural Networks”, Medical image analysis, Vol. 35, pp. 18-31, 2016.